

*Letter to the Editor***One more surprise from the Circinus Galaxy:  
BeppoSAX discovery of a transmission component in hard X-rays****G. Matt<sup>1</sup>, M. Guainazzi<sup>2</sup>, R. Maiolino<sup>3</sup>, S. Molendi<sup>4</sup>, G.C. Perola<sup>1</sup>, L.A. Antonelli<sup>5,6</sup>, L. Bassani<sup>7</sup>, W.N. Brandt<sup>8</sup>, A.C. Fabian<sup>9</sup>, F. Fiore<sup>5,6</sup>, K. Iwasawa<sup>9</sup>, G. Malaguti<sup>7</sup>, A. Marconi<sup>3</sup>, and J. Poutanen<sup>10</sup>**<sup>1</sup> Dipartimento di Fisica “E. Amaldi”, Università degli Studi “Roma Tre”, Via della Vasca Navale 84, I-00146 Roma, Italy<sup>2</sup> Astrophysics Division, Space Science Department of ESA, ESTEC, Postbus 299, 2200 AG Noordwijk, The Netherlands<sup>3</sup> Osservatorio Astrofisico di Arcetri, L.E. Fermi 5, I-50125 Firenze, Italy<sup>4</sup> Istituto di Fisica Cosmica e Tecnologie Relative, Via Bassini 15, I-20133 Milano, Italy<sup>5</sup> Osservatorio Astronomico di Roma, Via dell’Osservatorio, I-00044 Monteporzio-Catone, Italy<sup>6</sup> SAX/SDC Nuova Telespazio, Via Corcolle 19, I-00131 Roma, Italy<sup>7</sup> Istituto Tecnologie e Studio Radiazioni Extraterrestri, CNR, Via Gobetti 101, I-40129 Bologna, Italy<sup>8</sup> Department of Astronomy and Astrophysics, The Pennsylvania State University, University Park, PA 16802, USA<sup>9</sup> Institute of Astronomy, University of Cambridge, Madingley Road, Cambridge, CB3 0HA, UK<sup>10</sup> Stockholm Observatory, SE-133 36 Saltsjöbaden, Sweden

Received 27 October 1998 / Accepted 19 November 1998

**Abstract.** The Circinus Galaxy has been observed, for the first time above 10 keV, by BeppoSAX. An excess emission above the extrapolation of the best fit 0.1–10 keV spectrum is apparent in the PDS data. The most likely explanation is that we are observing the nucleus through a column density of  $\sim 4 \times 10^{24} \text{ cm}^{-2}$ , i.e. large enough to completely block the radiation below 10 keV but small enough to permit partial transmission above this energy.

**Key words:** X-rays: galaxies – galaxies: Seyfert – galaxies: individual: Circinus

**1. Introduction**

The Circinus Galaxy hosts one of the nearest Active Nuclei ( $d \sim 4 \text{ Mpc}$ ) and has been therefore much studied after its discovery (Freeman et al. 1977), despite the low Galactic latitude and therefore the relatively large interstellar absorption ( $N_{\text{H,Gal}} \sim 3 \times 10^{21} \text{ cm}^{-2}$ ).

The intense coronal lines (Oliva et al. 1994, Moorwood et al. 1996), the [O III] ionization cone (Marconi et al. 1994), the variable  $\text{H}_2$  maser emission (Greenhill et al. 1997), the broad  $\text{H}\alpha$  line in polarized light (Oliva et al. 1998a), and the reflection-dominated 2–10 keV X-ray spectrum (Matt et al. 1996, hereinafter M96) support the Seyfert 2 classification for the Circinus Galaxy. The integrated IR luminosity is about  $4 \times 10^{43} \text{ erg s}^{-1}$ , a large fraction of it being probably reprocessing of the nuclear radiation (Moorwood et al. 1996; Maiolino et al. 1998).

The ASCA observation (M96) revealed a flat X-ray spectrum with several emission lines, including a very prominent iron  $\text{K}\alpha$  line at about 6.4 keV. These findings were interpreted

by M96 in terms of reflection by cold matter (possibly the inner wall of the putative torus envisaged by unification models, e.g. Antonucci 1993) of an otherwise invisible nuclear emission. The absence of any transmitted component in the ASCA band (i.e. up to 10 keV) indicates a column density for the absorbing matter in excess of  $10^{24} \text{ cm}^{-2}$ , i.e. a Compton-thick source.

The Circinus Galaxy was observed by BeppoSAX (Boella et al. 1997) on 1998 March 24 as part of a Core Program aiming to study the broad band spectra of Compton-thick Seyfert 2 galaxies. Here we report on the spectral analysis of the source, with particular emphasis on the high energy part of the spectrum.

**2. Observation and data reduction**

We will discuss here data from three instruments: the LECS, the MECS and the PDS. The MECS is presently composed of two units (after the failure of a third one), working in the 1–10 keV energy range. At 6 keV, the energy resolution is  $\sim 8\%$  and the angular resolution is  $\sim 0.7 \text{ arcmin}$  (FWHM). The LECS has characteristics similar to that of the MECS in the overlapping band, but its energy band extends down to 0.1 keV. The PDS is a passively collimated detector (about  $1.5 \times 1.5$  degrees f.o.v.) working in the 13–200 keV energy range. The effective exposure time of the observation was  $1.37 \times 10^5 \text{ sec}$  (MECS),  $8.37 \times 10^4 \text{ sec}$  (LECS) and  $6.32 \times 10^4 \text{ sec}$  (PDS).

A second source is clearly visible in the LECS and MECS images at about  $5'$  from the Circinus Galaxy. This source was discovered by ASCA (M96), and is also present in the ROSAT HRI image (Ward 1998). The nominal positions of both sources, as measured by BeppoSAX, are shifted by the same amount (about  $2'$ ) and in the same direction with respect to the HRI positions (which in turn are consistent with the optical position,

for Circinus, and the ASCA position, for the second source). Only the Y and X startrackers, one gyro and the solar sensor were in use during the observation, but not the Z startracker, i.e. that coaligned with the telescopes. In this configuration, absolute position reconstruction can be in error up to  $3'$ . The second source is about 3.7 times fainter in both instruments. The spectrum may be well fitted either by a power law with  $\Gamma \sim 2.35$  and  $N_{\text{H}} \sim 1.3 \times 10^{22} \text{ cm}^{-2}$  or a plasma model with  $kT \sim 6 \text{ keV}$  and  $N_{\text{H}} \sim 3.4 \times 10^{21} \text{ cm}^{-2}$ . In both cases, the extrapolation to the PDS band lies more than two orders of magnitude below the data, and its contribution to the PDS data may be neglected. Of course, in principle the excess emission in the PDS band, described in Sect. 3, could be due to this source, if it is heavily absorbed ( $N_{\text{H}} \simeq 10^{24} \text{ cm}^{-2}$ ). This would imply a physical scenario similar, but much more extreme and then less plausible, to that discussed below for Circinus.

To avoid, as far as possible, contamination from the second source we extracted data for both the LECS and the MECS in  $2'$  radii centred on the source. The background subtraction was performed using blank sky spectra from the same region of the detector field of view. The resulting count rates are  $4.41(\pm 0.08) \times 10^{-2}$  in the LECS and  $1.050(\pm 0.009) \times 10^{-1}$  counts/s in the MECS. PDS data have been reduced following the standard procedures described in Matt et al. (1997). In addition, we employed crystal temperature dependent Rise Time thresholds, which lead to a reduction by a factor up to 50% of the instrumental background. The PDS count rate is  $2.01 \pm 0.04$  counts/s.

The spectra were fitted using the calibration matrices released on September 1997. In the fit procedure, the LECS normalization was left free to vary with respect to the MECS one, while the PDS normalization was fixed to 0.8 (Grandi et al. 1997). The residual uncertainty on the PDS absolute flux calibration ( $\simeq \pm 10\%$ ) does not affect substantially the following results. All quoted fluxes refer to the MECS. Errors correspond to 90% confidence level for two interesting parameters (i.e.  $\Delta\chi^2=4.61$ ).

Meaningful LECS and MECS light curves of the Circinus Galaxy cannot be easily constructed: due to the problems in the aspect reconstruction, a small extraction radius results in a fictitious variation of the count rate due to the wobbling; if a large extraction radius is instead chosen, the contamination from the second source is significant. In the latter case, a variation up to 10% on time scales of hours is observed in the MECS. If this is fully attributed to the second source, as should be if the interpretation of the Circinus spectrum below 10 keV as pure reflection component is correct, this would imply a  $\sim 50\%$  amplitude variations in this source. Finally, the PDS light curve is consistent with being constant (with a  $\sim 40\%$  upper limit to the variability amplitude).

### 3. Spectral analysis and results

We firstly analysed the spectrum below 10 keV, to verify the consistency with the ASCA results (M96). The spectrum is very flat with a huge iron  $K\alpha$  line, as observed by ASCA and interpreted

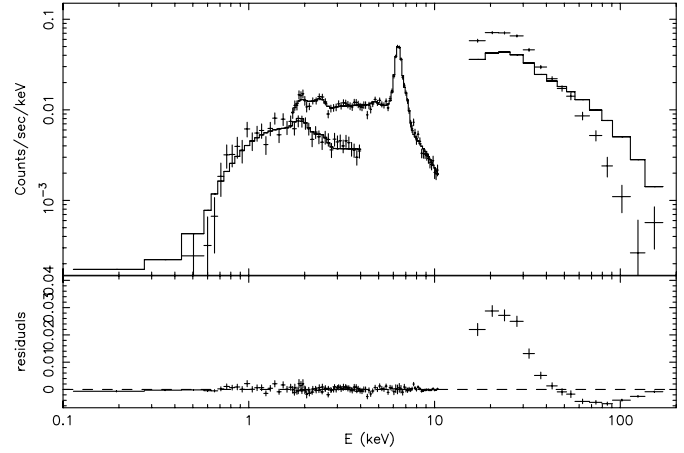


**Fig. 1.** LECS+MECS best fit model extrapolated to the PDS data. The model is composed by a pure reflection component ( $\Gamma_h=1.60$ ), a soft power law ( $\Gamma_s=1.45$ ) plus the emission lines.

by M96 as reflection dominated emission, the reflection probably occurring in circumnuclear matter (hereinafter identified, for simplicity, with the “torus” familiar from the unification models). The 2–10 keV flux is  $1.4 \times 10^{-11} \text{ erg cm}^{-2} \text{ s}^{-1}$ , consistent with the ASCA one. At least other five lines, to be identified with Si, S, Ar and Ni  $K\alpha$  and Fe  $K\beta$  lines, are required, as well as excess emission below a few keV. The properties of the emission lines, as well as of the soft excess, are discussed in detail elsewhere (Guinazzi et al., 1998).

When the model described above is extrapolated to the PDS band, a huge excess emission is apparent (see Fig. 1). No known bright sources are present in the field of view of the PDS. The Galactic longitude ( $311^\circ$ ) and latitude ( $-3.8^\circ$ ) of the source are about  $10^\circ$  outside the bulk of the Galactic Ridge emission (Warwick et al. 1985). Following the modelling of Yamasaki et al. (1997), we found that the contribution of the Galactic Ridge to the PDS count rate is at most 7%. Therefore, it is very likely that we are observing a further component in the Circinus spectrum, possibly the nuclear radiation piercing throughout a very large column density absorber, as in the case of NGC 4945 (Iwasawa et al. 1993; Done et al. 1996) and Mkn 3 (Cappi et al. 1998). In order to conceal itself below 10 keV, the absorber column density must exceed  $10^{24} \text{ cm}^{-2}$ , i.e. must be Compton-thick. This implies that the photons which eventually emerge may have suffered one or more Compton scatterings. We have therefore adopted a model, based on MonteCarlo simulations, which properly treats photon transfer in very high column density matter (work in preparation), including Compton downscattering and the Klein–Nishina decline. We assumed a spherical geometry as the simplest approximation of the (actually unknown) distribution of the matter. If a plane-parallel geometry, with normal illumination, is employed, the results do not change significantly.

We have then fitted the whole spectrum with the following model:

$$F(E) = [A_1 Tr(E, N_{\text{H},1}, \Gamma_h, E_c) + A_2 R(E, \Gamma_h, E_c) + A_3 E^{-\Gamma_s} + \text{emission lines}] e^{-N_{\text{H},2} \sigma_{\text{ph}}} \quad (1)$$

**Table 1.** Best fit parameters. See text for details on the models.

	1	2
$N_{H,1}$ ( $10^{24}$ cm $^{-2}$ )	$4.3^{+0.4}_{-0.7}$	$2.9^{+0.6}_{-0.7}$
$A_1$	$0.11^{+0.07}_{-0.08}$	$0.12^{+0.15}_{-0.08}$
$\Gamma_h$	$1.56^{+0.16}_{-0.51}$	$1.62^{+0.21}_{-0.43}$
$E_C$ (keV)	$56^{+8}_{-23}$	$81^{+37}_{-37}$
$A_2$	$2.02^{(+0.65)}_{(-0.98)} 10^{-2}$	$2.10^{(+0.68)}_{(-0.95)} 10^{-2}$
$\Gamma_s$	$1.64^{+0.13}_{-0.43}$	$1.60^{+0.18}_{-0.41}$
$A_3$	$8.3^{(+1.2)}_{(-1.7)} 10^{-4}$	$8.0^{(+1.4)}_{(-1.7)} 10^{-4}$
$N_{H,2}$ ( $10^{21}$ cm $^{-2}$ )	$3.6^{+1.0}_{-1.0}$	$3.5^{+1.1}_{-1.3}$
$\chi^2/\text{d.o.f.}$	122/121	119/121

where

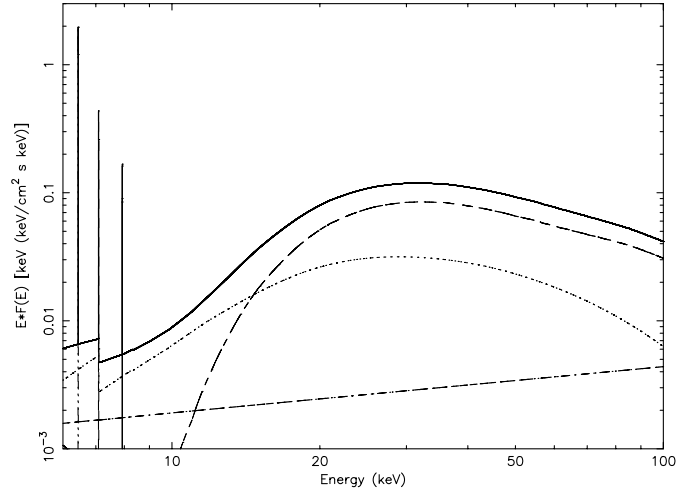
$$Tr = \int_E^\infty G(E, E_0, N_{H,1}) E_0^{-\Gamma_h} e^{-E_0/E_c} dE_0 \quad (2)$$

and  $G(E, E_0)$  is the Green function relating input and transmitted spectra.  $\Gamma_h$  and  $\Gamma_s$  are the power law indices of the hard (nuclear) component and of the soft component, respectively;  $N_{H,1}$  is the column density of the torus and  $N_{H,2}$  that of any external matter along the line of sight.  $R(E, \Gamma_h, E_c)$  is the pure reflection spectrum, obtained using PEXRAV in XSPEC fixing  $\cos(\theta)$  to 0.45 and `rel_refl` to -1.

The 20–100 (50–150) keV total flux is  $2.3 \times 10^{-10}$  ( $0.9 \times 10^{-10}$ ) erg cm $^{-2}$  s $^{-1}$ , which makes the Circinus Galaxy one of the brightest AGN in hard X-rays. The best fit parameters are summarized in Table 1 (model 1), while the best fit model is shown in Fig. 2.  $\Gamma_s$  and  $\Gamma_h$  are very similar, and consistent within the errors. It is possible that the soft emission is due to scattering of the nuclear radiation by ionized matter (Guainazzi et al. 1998).

The normalization of the nuclear component,  $A_1$ , is about 5 times larger than that of the reflection component,  $A_2$ ; therefore, the solid angle subtended by the reflecting matter to the nucleus and visible at infinity is  $\sim 0.2 \times 2\pi$ . Assuming a torus geometry like that adopted by Ghisellini et al. (1994) (i.e. a conical geometry with half-opening angle of 30°), we derive an inclination angle  $\lesssim 40^\circ$ .

The 2–10 keV nuclear luminosity, after correction for absorption, ranges from  $3.4 \times 10^{41}$  to  $1.7 \times 10^{42}$  erg s $^{-1}$  (assuming a distance of 4 Mpc). The IR luminosity (as defined by Mulchaey et al. 1994) is 20 to 100 times larger. This IR/(2–10 keV) ratio is somewhat higher than the average value for Seyfert galaxies, but by no means unique (see Fig. 2a of Mulchaey et al. 1994; Awaki 1997). If a significant fraction of the IR emission is reprocessing of the nuclear component, a large UV nuclear emission is implied, qualitatively in agreement with the calculations of Moorwood et al. (1996) and Oliva et al. (1998b) based on the IR lines. The X-ray to OIII ratio is typical for Seyfert galaxies (Bassani et al. 1998).

**Fig. 2.** Best fit reflection + transmission model (in  $\nu F_\nu$ ).

We have also tested a different scenario (model 2 in Table 1), in which the transmitted component is simply a fraction of the total reflection component, i.e. the reflecting matter is partially covered. This case would represent a scenario in which the line of sight towards the nucleus is completely blocked (i.e.  $N_H$  in excess of  $\sim 10^{25}$  cm $^{-2}$ ), but the optical depth diminishes at higher torus latitudes, so permitting transmission of some of the radiation reflected by the far side of the torus. The spectrum is similar to that of Eq. 1, but substituting, in the integral of Eq. 2, the reflection component to the power law one. From the statistical point of view, this model is as good as model 1. The  $A_1/A_2$  ratio is now the ratio between the solid angles subtended by the covered and uncovered matter to the source and visible at infinity. From Table 1, it can be seen that the covered fraction of the reflector is 5 times larger than the uncovered one. No estimate of the nuclear luminosity is possible in this model, and therefore no information on the torus geometry can be derived.

The observed value of the torus column density is  $4.3 \times 10^{24}$  cm $^{-2}$  in model 1 (and not much lower in model 2), i.e. about 350 times larger than the value expected from the extinction in the V band ( $A_V=5$  mags) measured from narrow lines Balmer decrement (Oliva et al. 1994) assuming a Galactic dust-to-gas ratio. Very likely, the absorbers responsible for the obscuration of the nucleus and the narrow line region are different, the former being distributed on much smaller scales. Granato et al. (1997) fitted the ISO spectrum (Moorwood et al. 1996) with their torus model, and found  $A_V=50$  mags for the torus, corresponding to a  $N_H$  more than one order of magnitude lower than our measured value, thus implying a dust depleted material. If their estimate is correct, the absorbing matter should then be located inside the dust sublimation radius which, given the nuclear luminosity derived from model 1, is of order of 0.01 pc, very close indeed to the central engine and suggestive of a possible identification of the absorbing material with the BLR.

Finally, a high energy cutoff with  $e$ -folding energy below 100 keV is required by the data in both models. This, together with the rather flat intrinsic power law, make Circinus similar,

as far as the primary spectral shape is concerned, to NGC 4151 (see e.g. Piro et al. 1998).

#### 4. Discussion

The main results of the BeppoSAX observation of the Circinus Galaxy can be summarized as follows:

I) The spectrum below 10 keV is dominated by a reflection component, in agreement with the ASCA result (M96).

II) The extrapolation of the LECS+MECS best fit spectrum falls short of the PDS data. A further component transmitted through a  $\sim 4 \times 10^{24} \text{ cm}^{-2}$  absorber is required, but it is not possible to establish, on statistical ground, whether we are looking at nuclear radiation or at a reflection component passing through the outer edge of the torus, even if the rather *ad hoc* geometry required in the second scenario makes the first hypothesis more appealing. To further address this issue, one has to search for short term variability, a task which requires much more sensitive hard X-ray detectors, like those on board Constellation-X. If the transmitted radiation is actually the nuclear one, by comparing the nuclear luminosity and that of the reflection component the inclination angle of the system is constrained to be less than  $40^\circ$ , if the torus geometry proposed by Ghisellini et al. (1994) is adopted.

Finally, it is worth noting that two of the nearest AGNs, the Circinus Galaxy and NGC 4945, both have absorbing matter with  $N_{\text{H}}$  between  $10^{24}$  and  $10^{25} \text{ cm}^{-2}$ , suggesting that this kind of source is rather common in the Universe. This is particularly interesting because with such an absorber most of the energy in the X-ray band comes out at a few tens of keV (Fig. 2), where the energy density of the Cosmic X-ray Background peaks.

*Acknowledgements.* We acknowledge the BeppoSAX SDC team for providing pre-processed event files and the support in data reduction. The following institutions are acknowledged for financial support:

Italian Space Agency (GM, GCP, RM, SM, FF, AM), ESA (MG, research fellowship), NASA (WNB, LTSA program), Royal Society (ACF), PPARC (KI).

#### References

- Antonucci R., 1993, *ARA&A* 31, 473  
 Awaki H., 1997, in "Emission Lines in Active Galaxies: New Methods and Techniques", ASP conf. series Vol 113, p. 44  
 Bassani L., Dadina M., Maiolino R., et al., 1998, *ApJS*, in press  
 Boella G., Butler R.C., Perola G.C., et al., 1997, *A&AS*, 112, 299  
 Cappi M., Bassani L., Comastri A., et al., 1998, *A&A*, submitted  
 Done C., Madejski G.M., Smith D.A., 1996, *ApJ*, 463, 63  
 Freeman K.C., Karlsson B., Lynga G., et al., 1977, *A&A*, 55, 445  
 Ghisellini G., Haardt F., Matt G., 1994, *MNRAS* 267, 743  
 Granato G.L., Danese L., Franceschini A., 1997, *ApJ*, 486, 147  
 Grandi P., Guainazzi M., Mineo T., et al., 1997, *A&A* 325, 17  
 Greenhill L.J., Ellingsen S.P., Norris R.P., et al., 1997, *ApJ*, 474, L103  
 Guainazzi M., Matt G., Bassani L., et al., 1998, in preparation  
 Iwasawa K., Koyama K., Awaki H., et al., 1993, *ApJ*, 409, 155  
 Yamasaki N.Y., Ohashi T., Takahara F., et al., 1997, *ApJ*, 821, 831  
 Maiolino R., Krabbe A., Thatte N., Genzel R., 1998, *ApJ*, 493, 650  
 Marconi A., Moorwood A.F.M., Origlia L., Oliva E., 1995, *ESO Messenger*, 78, 20  
 Matt G., Fiore F., Perola G.C., et al., 1996, *MNRAS*, 208, 253 (M96)  
 Matt G., Guainazzi M., Frontera F., et al., 1997, *A&A*, 325, L13  
 Moorwood A.F.M., Lutz D., Oliva E., et al., 1996, *A&A*, 315, L109  
 Mulchaey J.S., Koratkar A., Ward M.J., 1994, *ApJ*, 436, 586  
 Oliva E., Salvati M., Moorwood A.F.M., Marconi A., 1994, *A&A*, 288, 457  
 Oliva E., Marconi A., Cimatti A., di Serego Alighieri S., 1998a, *A&A*, 329, L21  
 Oliva E., Marconi A., Moorwood A.F.M., 1998b, *A&A*, in press (astro-ph 9811177)  
 Piro L., Nicastro F., Feroci M., et al., 1998, *Nucl. Phys. B (Proc. Suppl.)*, 69/1-3, 490  
 Ward M.J., 1998, "Science with XMM", First XMM workshop, October 1998  
 Warwick R.S., Turner M.J.L. Turner, Watson M.G., Willingale R., 1985, *Nat*, 317, 218